Journal of Applied Polymer Science

Preparation and Characterization of Polyamide 66/Poly(hydroxyl ether of bisphenol A) Blends Without Compatibilizer

Jingjing An,[1] Xinyu Cao,[1] Yongmei Ma,[1] Yucai Ke,[1] Huahao Yang,[1] Haiqiao Wang,[2] Fosong Wang[1]

[1]Key Laboratory of Green Printing, Institute of Chemistry, Chinese Academy of Sciences, Beijing 100190, People's Republic of China

[2]College of Materials Science and Engineering, Beijing University of Chemical Technology, Beijing 100029, People's Republic of China

Correspondence to: Y. Ma (E-mail: maym@iccas.ac.cn) or F. Wang (E-mail: wangfs@iccas.ac.cn)

ABSTRACT: The polyamide 66 (PA66)/poly(hydroxyl ether of bisphenol A) (PHE) blend was successfully prepared by twin-screw extrusion without the addition of any compatibilizer. The PA66/PHE blends had a microphase-separated structure that varied from a sea-island structure to a cocontinuous structure, and the mechanical properties were higher than the anticipated values on the basis of the rule of mixtures, which showed a synergistic effect. Fourier transform infrared spectroscopy and dynamic mechanical analysis illustrated that there was hydrogen-bonding interaction between the amide groups of the PA66 and the pendant hydroxyl groups of the PHE. This led to the some degree of compatibility and the improvement in the mechanical properties of the blends. The polarized optical microscopy observation showed that the PA66 spherulites of the blend became smaller and more imperfect compared to those of the pure PA66, and differential scanning calorimetry measurement also showed a decrease in the melting temperatures of PA66 of the blend. © 2014 Wiley Periodicals, Inc. J. Appl. Polym. Sci. **2014**, *131*, 40437.

KEYWORDS: blends; compatibilization; crystallization; mechanical properties

Received 6 June 2013; accepted 13 January 2014
DOI: 10.1002/app.40437

INTRODUCTION

The strength, stiffness, and toughness of polymers under their used conditions are obviously important in any structural application. Perhaps some of these properties can easily be modified in polymer blends. However, blends that have high strength, stiffness, and toughness properties are not easily obtained. For example, in rubber-toughened polymer blends, the rubber and so on may improve the toughness of the polymer matrix but at the sacrifice of its stiffness and strength.[1,2] Additionally, the fibers, rigid polymer components, and so on can improve the stiffness and strength of the polymer matrix, which may not be tough.[3,4] In 1984, Kurauche and Ohta[5] developed a new toughening concept, that is, a brittle, polymer-toughened ductile polymer matrix. Although the concept was based on a limited study on a plastic blend composed of a ductile matrix polycarbonate and dispersed brittle acrylonitrile–butadiene–styrene and poly(styrene-*co*-acrylonitrile) particles. Not long after, the concept was successfully extended to other polymer systems, and developments in multiphase alloys of two or more rigid polymers have led to a new generation of materials. The new multiphase alloys of rigid polymers usually have a high stiffness, strength, and toughness in their materials.[6–14] Until now, however, there has not been a successful example in polyamide/polymer alloys in which both components have been rigid polymers without any elastomeric phase at ambient temperature. Even in PA/Polyphenylene Oxide (PPO) and PA/acrylonitrile–butadiene–styrene blend systems with excellent mechanical properties, there has been a need for added compatibilizer[15–20] or the existence of an elastomeric phase.[17–20]

To achieve good mechanical properties in the polymer/polymer blends, some degree of interaction between the respective components is required. Polyamide 66 (PA66) is a widely used rigid engineering plastic with good strength and stiffness and a high crystallinity. Poly(hydroxyl ether of bisphenol A) (PHE) is an amorphous thermoplastic rigid polymer and has outstanding mechanical properties, such as toughness and dimensional stability. It has been reported that PHE is compatible with a number of polymers, including poly(ethylene oxide),[21] poly(ε-caprolactone),[22] poly(methyl methacrylate),[23] poly(vinyl pyrrolidone),[24] and others,[25–28] because of the formation of hydrogen-bonding interactions between the components. We concluded that there is a chance to form hydrogen-bonding interactions between the pendant hydroxyl groups of PHE and the amide groups of PA66 in the PA66/PHE blends (Figure 1)

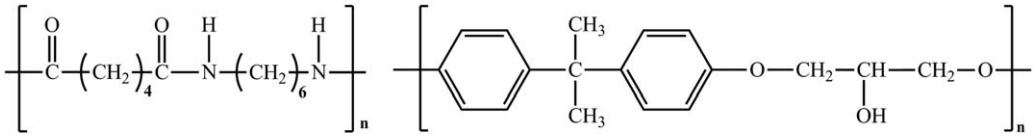

Figure 1. Chemical structures of PA66 and PHE.

and that this could enhance the compatibility and achieve good mechanical properties in the blends.

In this study, our interest was in the preparation of PA66/PHE blends without use of additional compatibilizer in which both components were rigid polymers at ambient temperature and in which the mechanical properties were evaluated. Meanwhile, we wanted to know about the hydrogen-bonding capacities in the blends and how they influenced the compatibility and the properties of the blends when hydrogen-bonding was present in this system. Therefore, the hydrogen-bonding interactions of the blends were expected to also be quite interesting. Moreover, this provided an important way to develop rigid–rigid polyamide alloys from the practical point of view.

In this study, we prepared the PA66/PHE blend without compatibilizer by twin-screw extrusion. The hydrogen-bonding interaction between PA66 and the PHE component was mainly investigated with Fourier transform infrared (FTIR) spectroscopy and dynamic mechanical analysis (DMA). The crystallization behavior, morphology, and mechanical properties of the blends were also characterized.

EXPERIMENTAL

Materials

PA66 (EPR27H, melting temperature = 262°C) was provided by China Shenma Group Co., Ltd. The PHE (number-average molecular weight = 21,497 g/mol, weight-average molecular weight/number-average molecular weight = 2.89) used in this study was prepared by our laboratory according to a Chinese patent.[29]

Blend Preparation

The PA66 samples were dried at 100°C for 14 h in a blast-drying oven, and the PHE samples were vacuum-dried at 65°C for 30 h before use. Blends with PA66/PHE weight radios of 100/0, 80/20, 60/40, 40/60, 20/80, and 0/100 were prepared by a twin-screw extruder at a screw speed of 250 rpm. The barrel temperatures were maintained at 100, 200, 270, 270, 270, 270, and 265°C. The blends produced were subsequently cut into pellets by a pelletizer. The extruded pellets were then dried in a vacuum oven at 80°C for 12 h and injection-molded into various standard test specimens with an injection-molding machine. The barrel temperatures were 245, 270, 270, and 245°C.

Characterization

FTIR spectra were recorded with a Tensor-27 (Bruker) spectrometer, and 32 scans were collected with a spectral resolution of 2 cm^{-1}. The testing range was from 400 to 4000 cm^{-1}. The samples were melted at 280°C, quickly cast on KBr discs, and finally put them in the vacuum desiccator before testing.

Differential scanning calorimetry (DSC) was used to investigate the crystallization behavior of both neat PA66 and its blends on a TA-Q100 instrument. The heating–cooling–heating cycles were

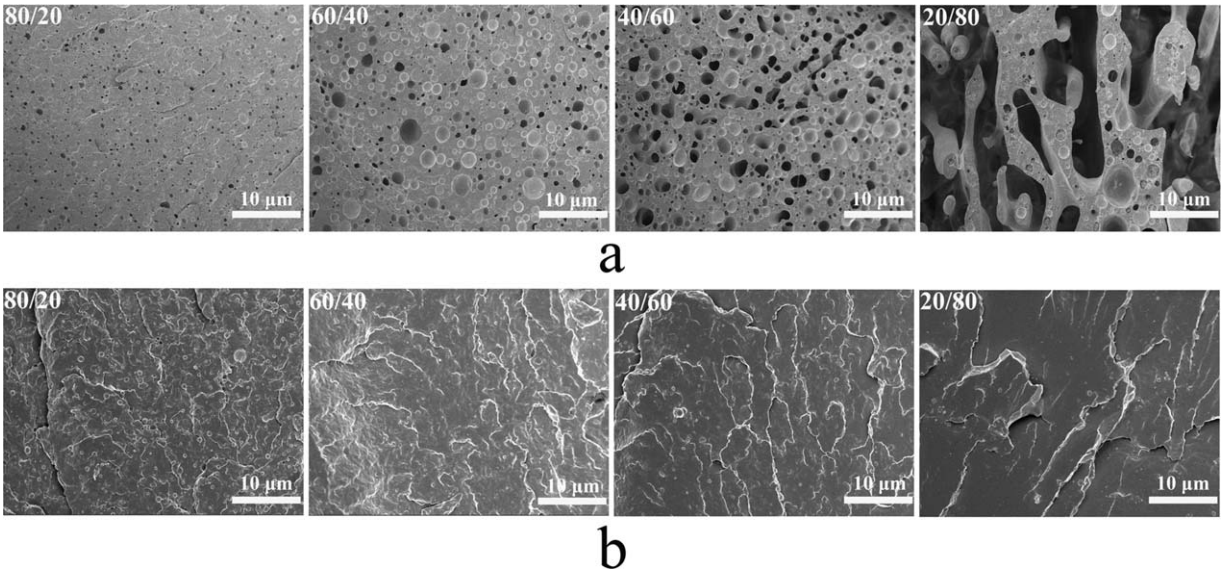

Figure 2. SEM micrographs of the cryofractured PA66/PHE blends with weight ratios of 80/20, 60/40, 40/60, and 20/80 (from left to right): (a) etched with THF and (b) not etched.

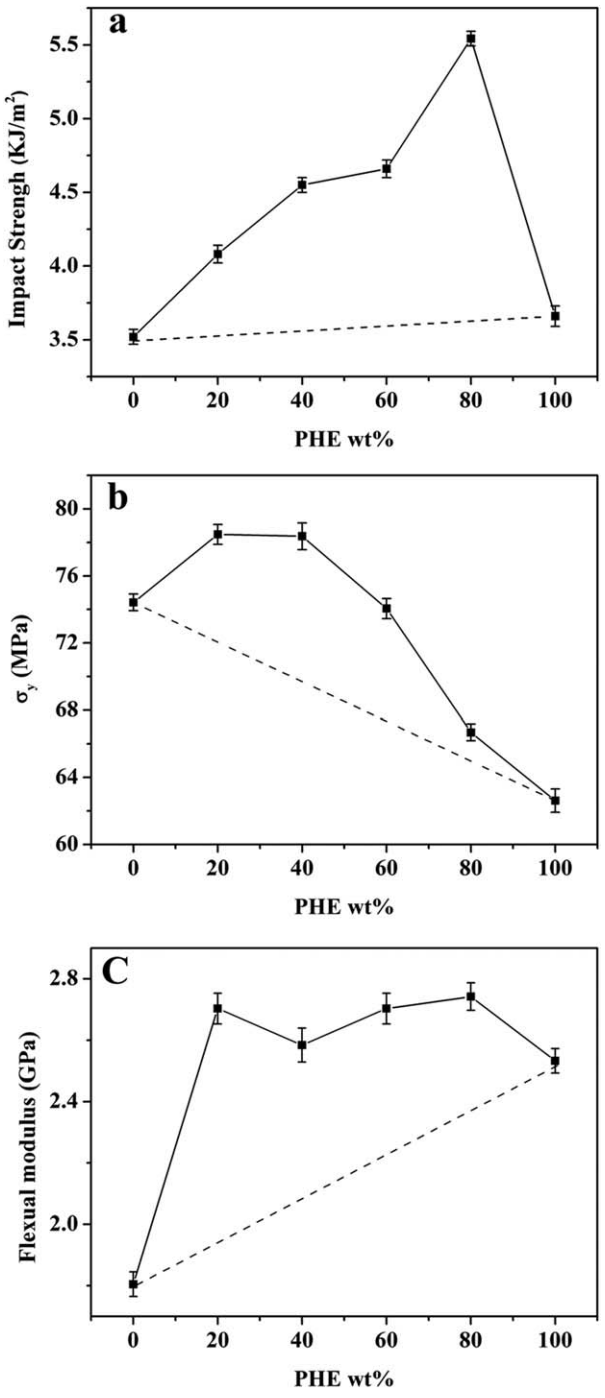

Figure 3. (a) Impact strength, (b) yield stress (σ_y), and (c) flexural modulus of the PA66/PHE blends versus the PHE content (the dashed lines represent the values predicted by the rule of mixture).

recorded in the temperature range 25–300°C at a scan rate of 20°C/min under a nitrogen atmosphere. In the first heating run, all of the samples were annealed at 300°C for 5 min to eliminate the thermal history.

DMA was used to investigate the dynamic mechanical properties of the blends by a TA-Q800 instrument operated in a single-cantilever clamp. The size of the specimens was 2 × 12 × 25 mm^3. The test samples were tested over a temperature range of −145°C to 150°C at a rate of 3°C/min and a frequency of 1 Hz.

Scanning electron microscopy (SEM) observations of the surfaces were produced by the cryofracturing of the samples in liquid nitrogen to produce virgin surface characteristics of the bulk morphology. Two kinds of specimens were observed: one was the nonetched specimen for the inspection of the interface between the components, and the other was etched with tetrahydrofuran (THF) to determine the morphology of the phases. All of the specimens were sputter-coated with gold–palladium

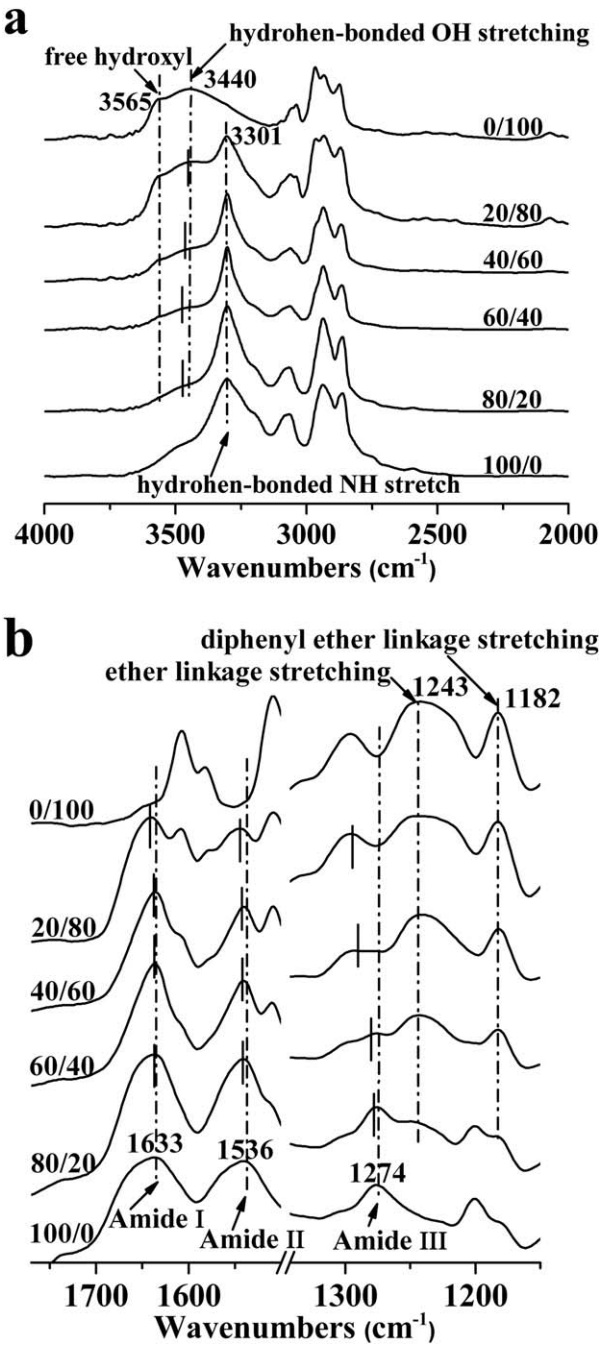

Figure 4. FTIR spectra of the PA66/PHE blends.

Table I. FTIR Band Assignments for Various Compositions

		Band position (cm−1)					
	Band assignment	100/0 PA66/PHE	80/20 PA66/PHE	60/40 PA66/PHE	40/60 PA66/PHE	20/80 PA66/PHE	0/100 PA66/PHE
PA66	Hydrogen-bonded N—H stretching	3301	3301	3301	3301	3301	—
	Stretching mode of C=O, amide I	1633	1638	1638	1638	1641	—
	N—H in-plane bending and C—N stretching, amide II	1536	1542	1542	1543	1545	—
	C—N—H stretching, amide III	1274	1278	1279	1289	1295	—
PHE	Free hydroxyl stretching	—	3565	3565	3565	3565	3565
	Hydrogen-bonded O—H stretching	—	3475	3469	3462	3451	3440
	Ether linkage stretching	—	1243	1243	1243	1243	1243
	Diphenyl ether linkage stretching	—	1182	1182	1182	1182	1182

for 2 min to produce a conductive coating and imaged with a JSM-6700F scanning electron microscope.

The crystalline morphologies of the blends were observed with polarized optical microscopy (POM; Olympus BX51-P system). The film samples (with a thickness of about 50 μm) were prepared by the melting (at 280°C for 5 min) and pressing small amounts of extruded neat PA66 and PA66/PHE blends (sandwiched between two microscope glass slides) and cooling at a rate of 20°C/min to 30°C.

To determine the mechanical strength of the blends, all of the specimens were inspected before the test, and any with obvious imperfections were discarded. The samples were vacuum-dried at 80°C for 30 h before the test. The Notched Izod impact measurements were measured with a Ceast pendulum impact strength tester CSI-137C at room temperature. The tensile and flexural properties were determined at ambient temperature with an Instron 3365 universal material testing machine with a speed of 50 and 2 mm/min, respectively, in compliance with the ISO standard, and the data were recorded as the average value of five parallel determinations.

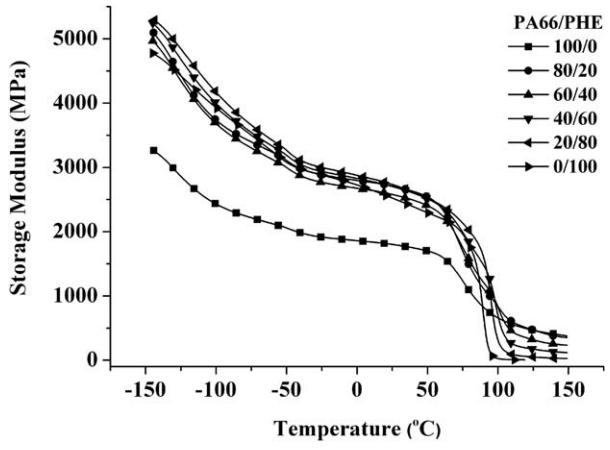

Figure 5. Temperature dependence of the storage modulus at 1 Hz for the PA66/PHE blends: (■) 100/0, (●) 80/20, (▲) 60/40, (▼) 40/60, (◀) 20/80, and (▶) 0/100.

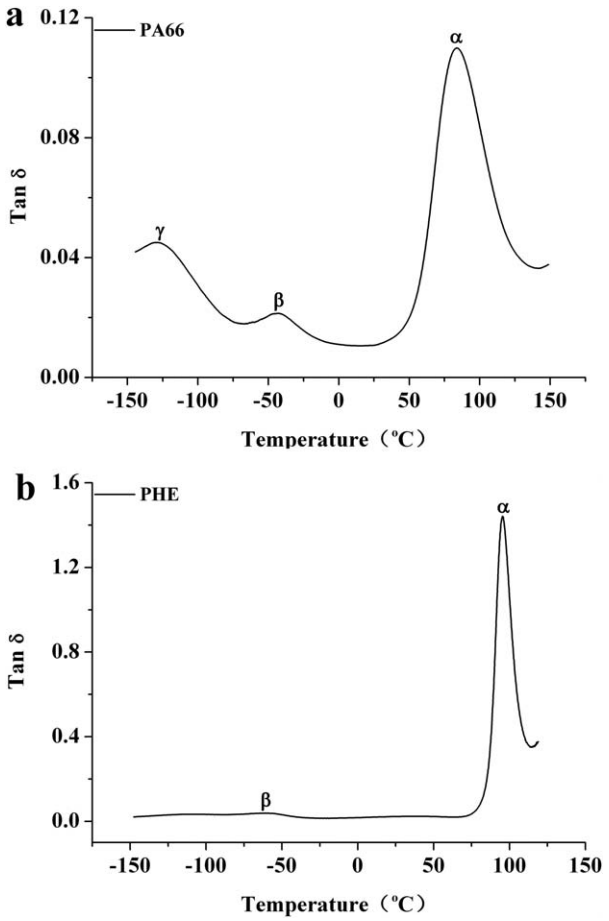

Figure 6. Temperature dependence of tan δ at 1 Hz: (a) PA66 (the α relaxation: the glass transition; the β relaxation: segmental motion of amide groups for non hydrogen bonding to other amides or a nearby chain; the γ relaxation: the crankshaft-like rotation of the methylene groups between the amide group.) and (b) PHE (the α relaxation: the glass transition; the β relaxation: the motion of the segment —CH_2—CH(OH)—CH_2—O—).

RESULTS AND DISCUSSION

SEM

The surface morphologies of the PA66/PHE blend with contents of PHE from 20 to 80 wt % are shown in Figure 2. The surface of the PA66/PHE blend was cryofractured and etched by THF, as shown Figure 2(a). The dark holes correspond to the PHE component in the blend that was etched by THF. Over the composition range, the blend had a two-phase structure, which varied from a sea-island structure to a cocontinuous structure when the content of PHE increased. This clearly indicated that it was not a completely compatible system.

The phase morphology of the PA66/PHE blends was related to the rheological aspects and shear stress, especially the interfacial tension between the individual polymers. As shown in Figure 2(b), the surface of the PA66/PHE blend was cryofractured without etching by THF, and the fracture surface of the blends did not show obvious holes and sharp interfaces at the boundary between the discrete phase and the continuous matrix. The results indicate that there was interaction between the components of the PA66/PHE blends, which decreased the interfacial free energy, and the boundaries of the two phases were obscure.

Mechanical Properties

The mechanical properties of the neat PA66, PHE, and PA66/PHE blends are shown in Figure 3. Apparently, the impact strength of the blends was higher than that of both neat PA66 and PHE over the entire composition range. When the PHE content was 80 wt %, the impact strength of blends was enhanced by 57% from 3.5 to 5.5 kJ/m^2 compared to that of neat PA66 [Figure 3(a)]. As shown in Figure 3(b), when the PHE content was lower than 60 wt %, the yield stress of the blend was higher than that of neat PA66, and when the PHE content was 40 wt %, the yield stress increased by 5%, from 74 to 78 MPa, compared with that of neat PA66. The flexural modulus of the PA66/PHE blend is shown in Figure 3(c). The flexural modulus of the blend was close to that of pure PHE and higher than that of pure PA66 over the entire composition range. This suggested that the introduction of PHE enhanced the stiffness of PA66. Moreover, the impact strength, yield stress, and flexural modulus of the blends were higher than their anticipated values on the basis of the rule of mixtures (dashed line). Hence, the synergistic effect[30–32] was present in the mechanical properties of the PA66/PHE blend. This also indicated that there was some degree of compatibility and interactions between the components.

FTIR Spectroscopy

Figure 4 shows the FTIR spectra of the PA66/PHE blends at room temperature in different components. The peak band and assignments for the PA66, PHE, and PA66/PHE blends are listed in Table I.

PA66 and PHE showed strong stretching absorptions at 3301 and 3565 cm^{-1}, respectively, as shown in Figure 4(a). The blends did not change these absorptions at 3301 cm^{-1}. However, the absorption band at 3440 cm^{-1} of the PHE component shifted to a higher wave number (by 35 cm^{-1}), and the shifting degrees gradually increased when the PA66 concentration was varied from 0 to 80 wt %. It was noted that PHE self-associates mainly through the strong intermolecular hydrogen bonding of

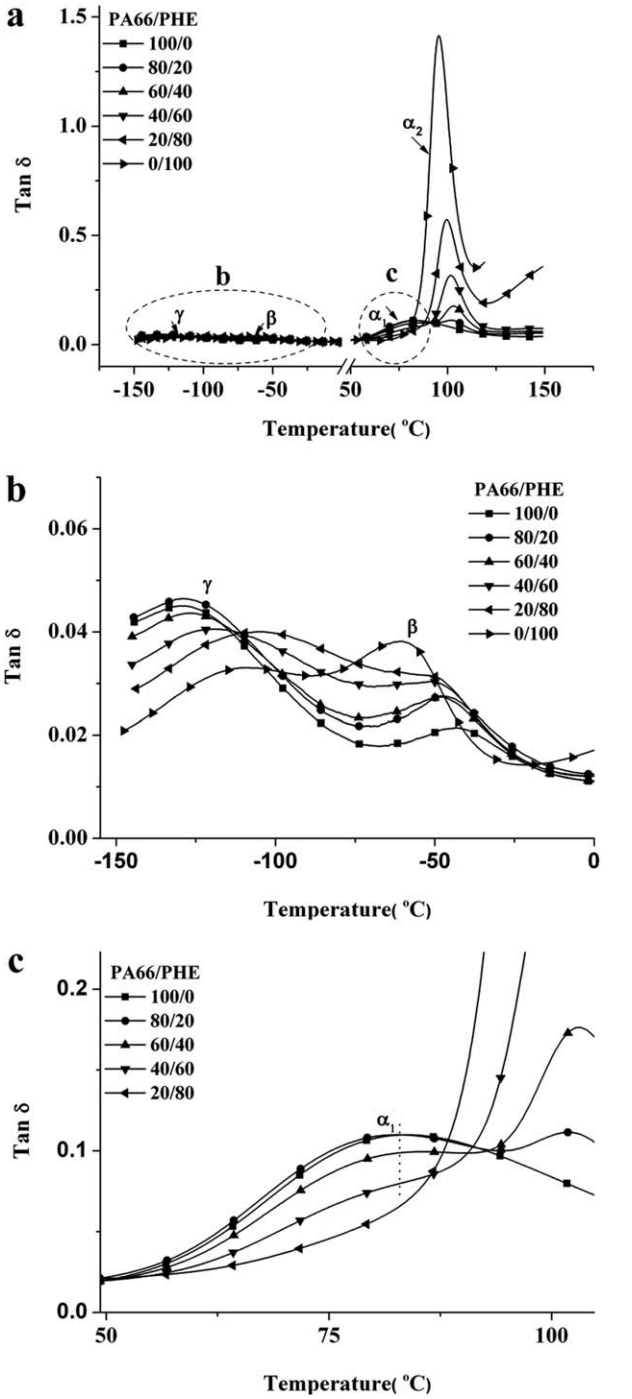

Figure 7. Temperature dependence of tan δ at 1 Hz for the PA66/PHE blends: (■) 100/0, (●) 80/20, (▲) 60/40, (▼) 40/60, (◀) 20/80, and (▶) 0/100.

the hydroxyl groups,[22] so it is reasonable to consider that the self-hydrogen bonds would be destroyed by the addition of PA66, and it implies that there exist interactions between PA66 and PHE in the blend.

As shown in Figure 4(b), pure PA66 shows strong amide group absorptions at 1633, 1536, and 1274 cm^{-1} attributed to amide I, amide II, and amide III (Table I), respectively. The

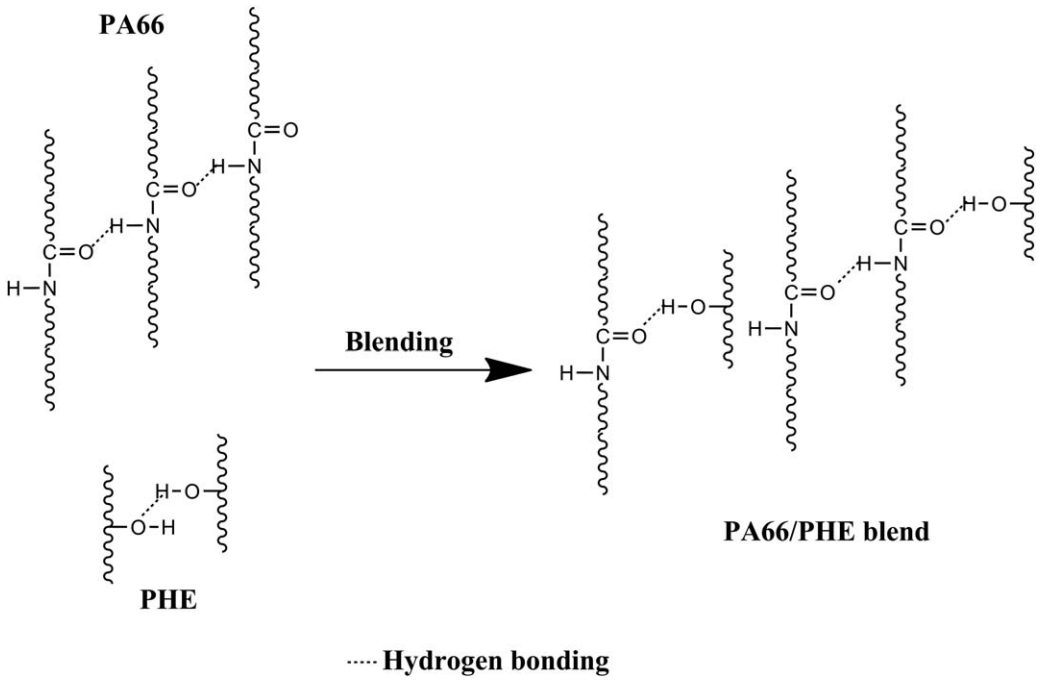

Figure 8. Scheme of the hydrogen-bonding interactions between PA66 and PHE.

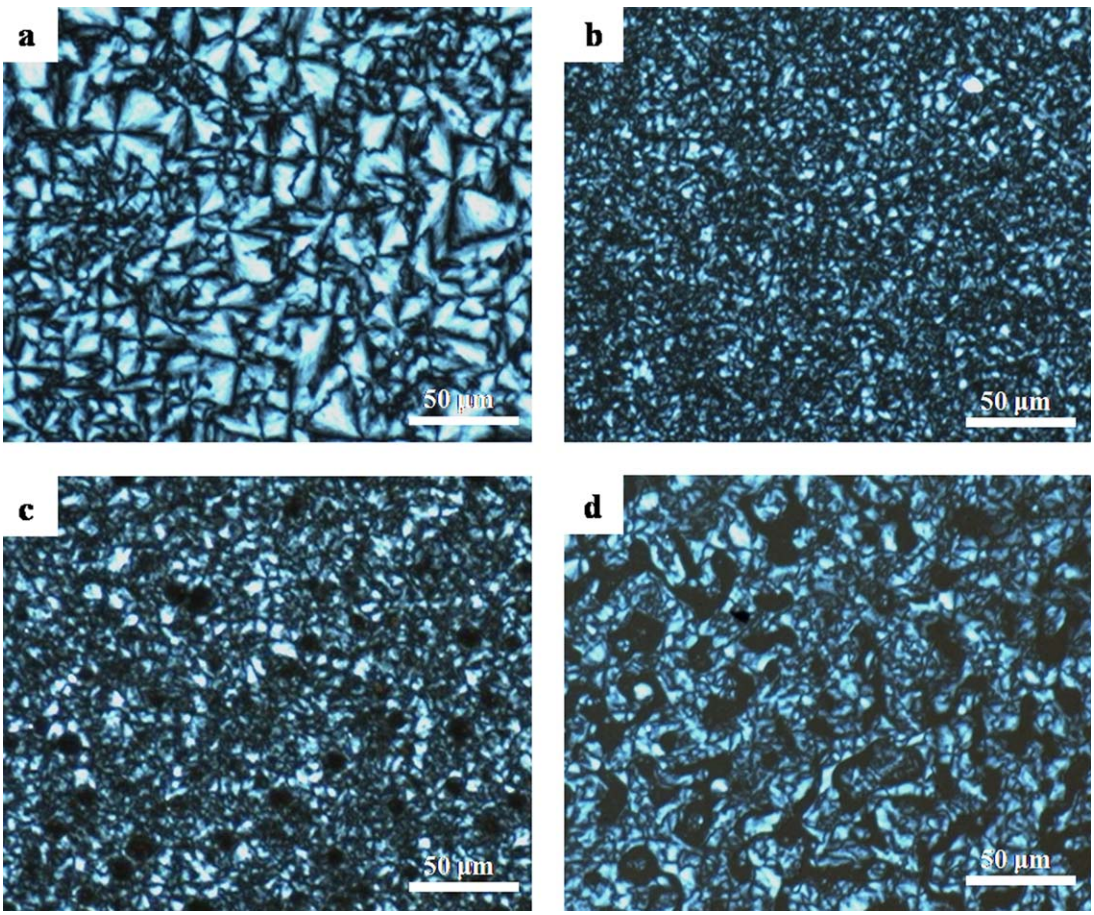

Figure 9. Crystalline morphologies of the PA66/PHE blends by POM: (a) 100/0, (b) 80/20, (c)60/40, and (d) 40/60. [Color figure can be viewed in the online issue, which is available at wileyonlinelibrary.com.]

amide I peak of PA66 at 1633 cm^{-1} shifted to a higher wave number (by 8 cm^{-1}) by the addition of PHE. Additionally, the other amide peaks of PA66 at 1536 and 1274 cm^{-1} also shifted to a higher wave number (by 9 and 21 cm^{-1}, respectively), and the degrees of shifting to higher frequencies of amide groups also gradually increased as the PHE concentration increased. This indicated that the original strong self-hydrogen bonding in the PA66 component was also destroyed by the addition of PHE.

Although the ether linkage stretching vibrations of PHE appeared at 1243 and 1182 cm^{-1}, respectively, they did not change their positions with decreasing PHE content, as shown in Figure 4(b). This means there was a lack of interactions between the ether linkages of the PHE and PA66 components.

The shifting of the amide bands of the PA66 and hydroxyl bands of PHE in the FTIR spectra indicated that the self-hydrogen bonding of both the PA66 and PHE components was destroyed, and the disassociated amide groups of PA66 should have interacted with the disassociated hydroxyl groups of PHE to form hydrogen bonding. It was proven by the DMA results. Such interactions contributed to the compatibility of the components and the enhanced mechanical properties of the blends.

DMA

The dynamic storage moduli as a function of temperature for the neat PA66, PHE, and PA66/PHE blends are shown in Figure 5. It shows that the storage moduli of the PA66/PHE blends were close to that of PHE but higher than that of PA66 with the addition of PHE in the wide temperature range below the glass transition. This indicated that the introduction of PHE enhanced the stiffness of PA66; this corresponded to the results of the moduli of the blends.

Three different relaxation processes (α, β, and γ) for PA66 are shown in Figure 6(a): (1) the α relaxation belonged to the glass transition and was connected to the cooperative mobility of the 25–50-atom chain, (2) the β relaxation was attributed to the segmental motion of amide groups for no-hydrogen bonding to other amides or a nearby chain, and (3) the γ relaxation was a result of the crankshaftlike rotation of the methylene groups between the amide groups.[33,34]

PHE had two different relaxations [α and β; Figure 6(b)]. The α and β relaxations were attributed to the glass transition and the motion of the —CH_2—CH(OH)—CH_2—O— segment, respectively.[35,36]

The PA66/PHE blends had two glass-transition temperatures (T_g's; T_{g1} and T_{g2}), as shown in Figure 7(a). T_{g1} of the blends was almost the same in comparison with that of pure PA66 [Figure 7(c)], and T_{g2} was enhanced with increasing PA66 and was about 9°C higher than that of pure PHE. We considered that the reason was that in microphase-separated PA66/PHE blend systems, when the crystallization temperature (T_c) of PA66 was higher than the T_g of PHE, during the cooling process, PA66 crystallized at T_c with an associated volume reduction, whereas the PHE was still in the liquid state. The liquid polymer was compressed (which was positive pressure, not negative pressure) with a resulting elevated T_g due to the well-known pressure dependence of T_g.[37–39]

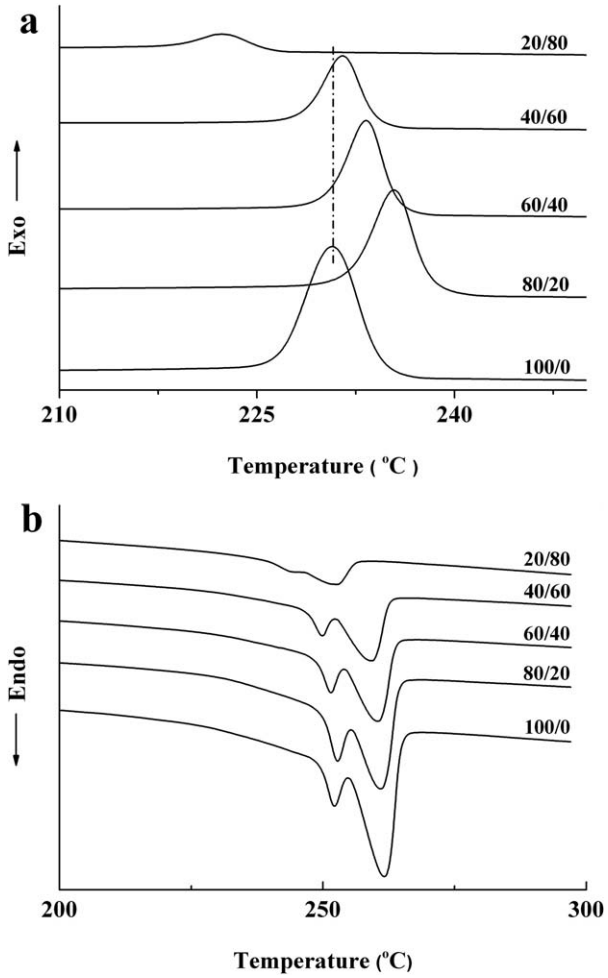

Figure 10. DSC curves of the PA66 and PA66/PHE blends: (a) upon cooling and (b) upon second heating.

For all of the blends of PA66/PHE, only single β peaks appeared between that of the pure PA66 (−41°C) and that of the pure PHE (−59°C), as shown in Figure 7(b). Some researchers[34] reported that the chemical reactions or the formation of hydrogen bonding between the amide groups and other groups made the β transition of polyamide disappear in the blends. We speculated that the β transition of the PA66/PHE blends was the motion of the —CH_2—CH(OH)—CH_2—O— segment of the PHE component. Due to the formation of hydrogen bonding between the hydroxyl groups on the —CH_2—CH(OH)— CH_2—O— segment of PHE and the amide groups of PA66 in the blends (Figure 8), the β-transition temperature of the PA66 component disappeared. Meanwhile, the motion of that of PHE component became difficult and shifted to a higher temperature with increasing PA66 because of the hydrogen-bonding interactions.

The γ peak of the PA66/PHE blends shifted to a temperature higher than that of the pure PA66, as shown in Figure 7(b). This was due to the existence of hydrogen bonding between the components and the introduction of benzene rings of the PHE component, which hindered the motion of methylene groups.

The DMA results of the PA66/PHE blends proved that there were hydrogen-bonding interactions between the PA66 and PHE components, and this contributed to the compatibility of the two components and the excellent properties of the blend. Unlike the blends of PHE with polymers such as poly(ethylene oxide)[21] or poly(ε-caprolactone),[22] where the two polymers are completely miscible in one another, primarily because of the formation of strong hydrogen bonds between the intermolecular segments of the components, and only a single T_g appeared. The blends of PA66 and PHE were partially compatible, and two phases existed. They had two T_g's.

POM

The POM micrographs of the neat PA66 and PA66/PHE blends are shown in Figure 9. Typical and well-developed crystal spherulites with a size of about 30–50 μm were inhomogeneously dispersed in neat PA66. After the addition of PHE, the spherulites of PA66 became more imperfect and smaller, especially for those domains near the PHE phases, because of the existence of hydrogen bonding between the two components. This inhibited the molecular chains of PA66 folding to form large crystals and also meant that PHE acted as a nucleation agent for PA66. Moreover, we also observed that there was the phase inversion of the PA66/PHE blends from small discrete regions of PHE to cocontinuous blends at higher PHE levels (the black area in Figure 9); this corresponded to the results of SEM.

DSC

The DSC curves of PA66 and its blends are presented in Figure 10. The thermograms clearly indicate that PHE raised the rate of nucleation or the crystallization of PA66 because the T_c's increased except in the blend with 80 wt % PHE [Figure 10(a)]. Figure 10(b) shows that the endothermic peaks of all of the samples exhibited double peaks upon their second heating.[40] This resulted from the existence of different sized spherulites, as revealed by POM. For blend samples due to the diluted effect and interaction between PA66 and PHE, the melting temperatures of the PA66 component decreased when the content of PHE was greater than 60 wt %. The crystallization degree of PA66 in the blends (ca. 48%) was almost the same in comparison with that of pure PA66 (45%).

CONCLUSIONS

Without any compatibilizer, the extruded microphase structured PA66/PHE blends with much enhanced mechanical properties were successfully prepared. PA66 and PHE were partially compatible, and this was attributed to the formation of hydrogen bonding between the pendant hydroxyl groups of PHE and the amide groups of PA66. It also led to an enhanced modulus, yield stress, and impact strength in the PA66/PHE blends. Additionally, the PA66 spherulites in the blends became smaller and more imperfect when the PHE content increased. The melting temperatures of the blends also decreased compared to the pure PA66. This work offers a very important way to develop rigid–rigid polyamide alloys from the practical point of view.

ACKNOWLEDGMENTS

The authors acknowledge support from the National Nature Science Foundation of China (NSFC) (contract grant number 51073163) and the Ministry of Science and Technology (MoST) 973 Research Program (contract grant number 2012CB933801).

REFERENCES

1. Borggreve, R. J. M.; Gaymans, R. J.; Eichenwald, H. M. *Polymer* **1989**, *30*, 78.
2. Bartczak, Z.; Argon, A. S.; Cohen, R. E.; Weinberg, M. *Polymer* **1999**, *40*, 2331.
3. Evans, A. G.; Zok, F. W. *J. Mater. Sci.* **1994**, *29*, 3857.
4. Thwe, M. M.; Liao, K. *Compos. A* **2002**, *33*, 43.
5. Kurauchi, T.; Ohta, *J. Mater. Sci.* **1984**, *19*, 1699.
6. Angola, J. C.; Fujita, Y.; Sakai, T.; Inoue, T. *J. Polym. Sci. Part B: Polym. Phys.* **1988**, *26*, 807.
7. Sue, H. J.; Pearson, R. A.; Yee, A. F. *Polym. Eng. Sci.* **1991**, *31*, 793.
8. Guo, Q. P.; Huang, J. Y.; Li, B. Y.; Chen, T. L.; Zhang, H. F.; Feng, Z. L. *Polymer* **1991**, *32*, 58.
9. Kyu, T.; Saldanha, J. M.; Kiesel, M. J. Two-Phase Polymer Systems; Hanser: Munich, **1991**.
10. Nassar, T. R.; Paul, D. R.; Barlow, J. W. *J. Appl. Polym. Sci.* **1979**, *23*, 85.
11. Murff, S. R.; Barlow, J. W.; Paul, D. R. *J. Appl. Polym. Sci.* **1984**, *29*, 3231.
12. Koo, K. K.; Inoue, T.; Miyasaka, K. *Polym. Eng. Sci.* **1985**, *25*, 741.
13. Choi, C. H.; Lee, S. M.; Kim, B. K. *J. Macromol. Sci. Phys.* **1994**, *33*, 317.
14. Wu, J. S.; Mai, Y. W.; Yee, A. F. *J. Macromol. Sci.* **1994**, *29*, 4510.
15. Zhang, T. T.; Li, Y.; Qu, X. W. *Key Eng. Mater.* **2012**, *501*, 99.
16. Chiang, C. R.; Chang, F. C. *Polymer* **1997**, *38*, 4807.
17. Sue, H. J.; Yee, A. F. *J. Mater. Sci.* **1989**, *24*, 1447.
18. Yang, H. H.; Cao, X. Y.; Ma, Y. M.; An, J. J.; Ke, Y. C.; Liu, X. M.; Wang, F. S. *Polym. Eng. Sci.* **2012**, *52*, 481.
19. Araujo, E. M.; Hage, E., Jr.; Carvalho, A. J. F. *J. Appl. Polym. Sci.* **2003**, *90*, 2643.
20. Xu, X. Y.; Sun, S. L.; Chen, Z. C.; Zhang, H. X. *J. Appl. Polym. Sci.* **2008**, *109*, 2482.
21. Iriarte, M.; Espi, E.; Etxeberria, A.; Valero, M.; Fernindezberridi, M. J.; Iruin, J. J. *Macromolecules* **1991**, *24*, 5546.
22. Coleman, M. M.; Moskala, E. *J. Polymer* **1983**, *24*, 251.
23. Kim, B. K.; Choi, C. H. *Polymer* **1996**, *37*, 807.
24. Martinez de Ilarduya, A.; Iruin, J. J.; Fernandez-Berridi, M. J. *Macromolecules* **1995**, *28*, 3707.
25. Wu, C. P.; Wu, Y. L.; Zhang, R. Y. *Eur. Polym. J.* **1998**, *34*, 1261.
26. Lau, C.; Zheng, S. X.; Zhong, Z. K.; Mi, Y. L. *Macromolecules* **1998**, *31*, 7291.
27. Zheng, S. X.; Mi, Y. L. *Polymer* **2003**, *44*, 1067.
28. Hameed, N.; Guo, Q. P. *Polymer* **2008**, *49*, 922.
29. Tan, X.; Luo, G. Q.; Lin, Z. R. (Guangzhou Research & Design Institute of Chemical Industry). Chin. Pat. 1,151,415 (**1997**).

30. Kolarik, J.; Lednicky, F.; Pukanszky, B.; Pegoraro, M. *Polym. Eng. Sci.* **1992**, *32*, 886.
31. Ma, X. F.; Yu, J. G.; Wang, N. *J. Polym. Sci. Part B: Polym. Phys.* **2006**, *44*, 94.
32. Hara, M.; Sauer, J. A. *J. Macromol. Sci. Rev. Macromol. Chem.* **1998**, *38*, 327.
33. Woodward, A. E.; Sauer, J. A.; Deeley, C. W.; Kline, D. E. *J. Colloid Sci.* **1957**, *12*, 363.
34. Han, C. D.; Chuang, H. K. *J. Appl. Polym. Sci.* **1985**, *30*, 2431.
35. Pogany, G A. *Polymer* **1970**, *11*, 66.
36. McCrum, N. G. A Review of the Science of Fibre Reinforced Plastics; Her Majesty's Stationery Office: London, **1971**.
37. Thirtha, V.; Lehman, R.; Nosker, T. *Polym. Eng. Sci.* **2005**, *45*, 1187.
38. Thirtha, V.; Lehman, R.; Nosker, T. *Polymer* **2006**, *47*, 5392.
39. Donth, E. The Glass Transition: Relaxation Dynamic in Liquid and Disordered Materials; Springer-Verlag: New York, **2001**.
40. Lee, S. S.; Phillips, P. *J. Eur. Polym. J.* **2007**, *43*, 1933.